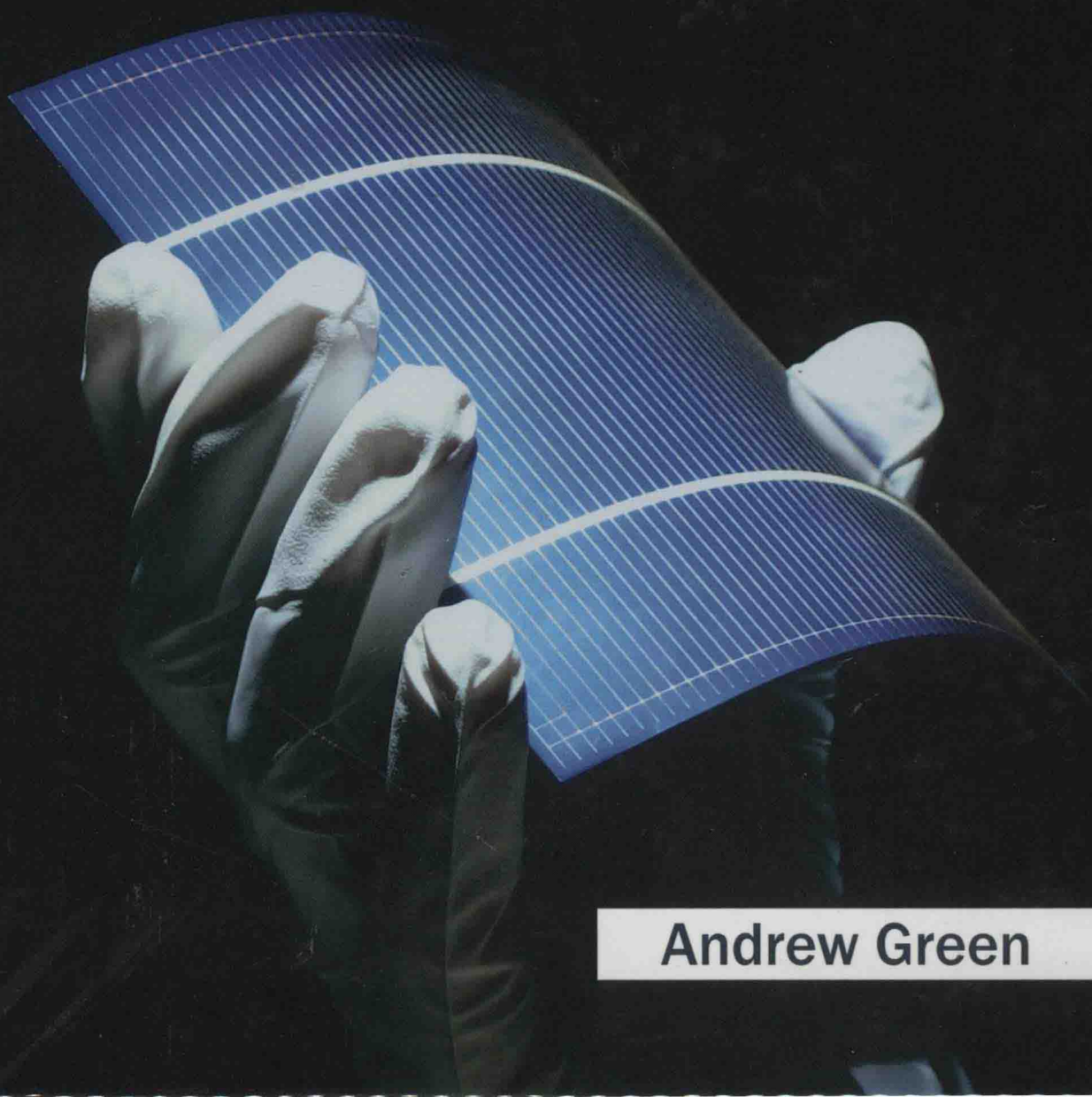


Advances in Nanotechnology

Volume I

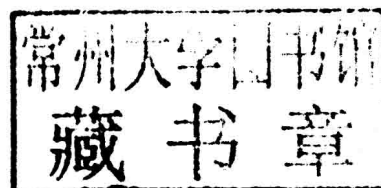


Andrew Green

Advances in Nanotechnology

Volume I

Edited by **Andrew Green**



NYRESEARCH
P R E S S

New York

Published by NY Research Press,
23 West, 55th Street, Suite 816,
New York, NY 10019, USA
www.nyresearchpress.com

Advances in Nanotechnology: Volume I
Edited by Andrew Green

© 2015 NY Research Press

International Standard Book Number: 978-1-63238-035-7 (Hardback)

This book contains information obtained from authentic and highly regarded sources. Copyright for all individual chapters remain with the respective authors as indicated. A wide variety of references are listed. Permission and sources are indicated; for detailed attributions, please refer to the permissions page. Reasonable efforts have been made to publish reliable data and information, but the authors, editors and publisher cannot assume any responsibility for the validity of all materials or the consequences of their use.

The publisher's policy is to use permanent paper from mills that operate a sustainable forestry policy. Furthermore, the publisher ensures that the text paper and cover boards used have met acceptable environmental accreditation standards.

Trademark Notice: Registered trademark of products or corporate names are used only for explanation and identification without intent to infringe.

Printed in China.

Advances in Nanotechnology

Volume I

Preface

This book is a compilation of research material on the emerging field of Nanotechnology. Engineering of functional systems at the molecular scale is referred to as nanotechnology or nanotech. Both the current work and advanced concepts related to this field are covered in this book. Nanotechnology is a technique used to construct an item using the bottoms up approach with high atomic precision. Today, by utilizing the technological advancement and techniques available in the field of nanotechnology, high performance products can be developed.

According to Feynman's vision of miniature factories, to build complex products using nanomachines, advanced nanotechnology should utilize positionally-controlled mechanochemistry guided by molecular machine systems. Nanotechnology is used in various fields of science these days. It plays a key role in areas such as medicine sciences, biotechnology etc. Besides, other applications include green nanotechnology, energy applications of nanotechnology and carbon tube related applications among numerous others.

This book provides a variety of researches and studies based on nanotechnology. It also covers some of the emerging aspects in the field of nanotechnology. I wish to thank all the authors for their efforts and time that they have given to this project. Without their dedication and timely submissions, this publication wouldn't have been possible. I must also acknowledge the editor and the team at the publishing house, who have done a tremendous job. Last but not the least, I wish to thank my family and friends, who have supported me in my life through everything. This book is meant for students, researchers, scientists, and for all those who want to learn and explore this interesting field of science.

Editor

Contents

	Preface	IX
Chapter 1	Raman Laser Polymerization of C₆₀ Nanowhiskers Ryoei Kato and Kun'ichi Miyazawa	1
Chapter 2	Characterization of Titanium Oxide Nanoparticles Obtained by Hydrolysis Reaction of Ethylene Glycol Solution of Alkoxide Naofumi Uekawa, Naoya Endo, Keisuke Ishii, Takashi Kojima and Kazuyuki Kakegawa	7
Chapter 3	Large-Scale Atmospheric Step-and-Repeat UV Nanoimprinting Kentaro Ishibashi, Hiroshi Goto, Jun Mizuno and Shuichi Shoji	15
Chapter 4	Nanostructured Porous Silicon Photonic Crystal for Applications in the Infrared G. Recio-Sánchez, V. Torres-Costa, M. Manso-Silván and R. J. Martín-Palma	24
Chapter 5	Mechanical and Thermal Characteristics of Bio-Nanocomposites Consisting of Poly-L-lactic Acid and Self-Assembling Siloxane Nanoparticles with Three Phases Masatoshi Iji and Naoki Morishita	30
Chapter 6	Electrospun Polyvinylpyrrolidone-Based Nanocomposite Fibers Containing (Ni_{0.6}Zn_{0.4})Fe₂O₄ W. S. Khan, R. Asmatulu, Y. H. Lin, Y. Y. Chen and J. C. Ho	38
Chapter 7	Chitosan/Carboxymethylcellulose/Ionic Liquid/Ag(0) Nanoparticles Form a Membrane with Antimicrobial Activity Camila Quadros, Vinícius W. Faria, Manuela P. Klein, Plinho F. Hertz and Carla W. Scheeren	43
Chapter 8	Nanotechnological Strategies for Biofabrication of Human Organs Rodrigo A. Rezende, Fábio de Souza Azevedo, Frederico David Pereira, Vladimir Kasyanov, Xuejun Wen, Jorge Vicente Lopes de Silva and Vladimir Mironov	52
Chapter 9	Henna (<i>Lawsonia inermis</i> L.) Dye-Sensitized Nanocrystalline Titania Solar Cell Khalil Ebrahim Jasim, Shawqi Al-Dallal and Awatif M. Hassan	62

Chapter 10	Fabrication of Axial and Radial Heterostructures for Semiconductor Nanowires by Using Selective-Area Metal-Organic Vapor-Phase Epitaxy	68
	K. Hiruma, K. Tomioka, P. Mohan, L. Yang, J. Noborisaka, B. Hua, A. Hayashida, S. Fujisawa, S. Hara, J. Motohisa and T. Fukui	
Chapter 11	Surface-Enhanced Raman Spectroscopy of Dye and Thiol Molecules Adsorbed on Triangular Silver Nanostructures: A Study of Near-Field Enhancement, Localization of Hot-Spots and Passivation of Adsorbed Carbonaceous Species	97
	Manuel R. Gonçalves, Fabian Enderle and Othmar Marti	
Chapter 12	The Effect of Solvents, Acetone, Water and Ethanol, on the Morphological and Optical Properties of ZnO Nanoparticles Prepared by Microwave	112
	Phindile B. Khoza, Makwena J. Moloto and Lucky M. Sikhwivhilu	
Chapter 13	<i>In Situ</i> Chemical Oxidation of Ultrasmall MoO_x Nanoparticles in Suspensions	118
	Yun-Ju Lee, Diego Barrera, Kaiyuan Luo and Julia W. P. Hsu	
Chapter 14	Uptake of Single-Walled Carbon Nanotubes Conjugated with DNA by Microvascular Endothelial Cells	123
	Joseph Harvey, Lifeng Dong, Kyoungtae Kim, Jacob Hayden and Jianjie Wang	
Chapter 15	Nanostructural Features of Silver Nanoparticles Powder Synthesized through Concurrent Formation of the Nanosized Particles of Both Starch and Silver	130
	A. Hebeish, M. H. El-Rafie, M. A. El-Sheikh and Mehrez E. El-Naggar	
Chapter 16	Investigating the Effect of In Ovo Injection of Silver Nanoparticles on Fat Uptake and Development in Broiler and Layer Hatchlings	140
	Lane Pineda, André Chwalibog, Ewa Sawosz, Anna Hotowy, Jan Elnif and Filip Sawosz	
Chapter 17	Fabrication of Bi-Doped TiO₂ Spheres with Ultrasonic Spray Pyrolysis and Investigation of Their Visible-Light Photocatalytic Properties	147
	Jianhui Huang, Wahkit Cheuk, Yifan Wu, Frank S. C. Lee and Wingkei Ho	
Chapter 18	Self-Organization of K⁺-Crown Ether Derivatives into Double-Columnar Arrays Controlled by Supramolecular Isomers of Hydrogen-Bonded Anionic Biimidazolate Ni Complexes	154
	Makoto Tadokoro, Kyosuke Isoda, Yasuko Tanaka, Yuko Kaneko, Syoko Yamamoto, Tomoaki Sugaya and Kazuhiro Nakasuji	
Chapter 19	Responses of Algal Cells to Engineered Nanoparticles Measured as Algal Cell Population, Chlorophyll a and Lipid Peroxidation: Effect of Particle Size and Type	164
	D. M. Metzler, A. Erdem, Y. H. Tseng and C. P. Huang	

Chapter 20	Immunocompatibility of Bacteriophages as Nanomedicines Tranum Kaur, Nafiseh Nafissi, Olla Wasfi, Katlyn Sheldon, Shawn Wettig and Roderick Slavcev	176
Chapter 21	Growth, Structural and Optical Characterization of ZnO Nanotubes on Disposable-Flexible Paper Substrates by Low-Temperature Chemical Method M. Y. Soomro, I. Hussain, N. Bano, Jun Lu, L. Hultman, O. Nur and M. Willander	189
Chapter 22	Surface-Enhanced Raman Scattering of Bacteria in Microwells Constructed from Silver Nanoparticles Mustafa Çulha, M. Müge Yazıcı, Mehmet Kahraman, Fikrettin Şahin and Sesin Kocagöz	195

Permissions

List of Contributors

Raman Laser Polymerization of C₆₀ Nanowhiskers

Ryoei Kato and Kun'ichi Miyazawa

National Institute for Materials Science, Fullerenes Engineering Group, 1-1, Namiki, Ibaraki, Tsukuba 305-0044, Japan

Correspondence should be addressed to Kun'ichi Miyazawa, miyazawa.kunichi@nims.go.jp

Academic Editor: Junfeng Geng

Photopolymerization of C₆₀ nanowhiskers (C₆₀NWs) was investigated by using a Raman spectrometer in air at room temperature, since the polymerized C₆₀NWs are expected to exhibit a high mechanical strength and a thermal stability. Short C₆₀NWs with a mean length of 4.4 μm were synthesized by LLIP method (liquid-liquid interfacial precipitation method). The A_g(2) peak of C₆₀NWs shifted to the lower wavenumbers with increasing the laser beam energy dose, and an energy dose more than about 1520 J/mm² was found necessary to obtain the photopolymerized C₆₀NWs. However, excessive energy doses at high-power densities increased the sample temperature and lead to the thermal decomposition of polymerized C₆₀ molecules.

1. Introduction

C₆₀ nanowhiskers (C₆₀NWs) are the single crystal nanofibers composed of C₆₀ molecules [1] and can be synthesized by a facile method called "LLIP method" [2]. C₆₀NWs have a variety of applications and such as field-effect transistors (FETs) [3], solar cells [4], biosensors [5].

C₆₀ molecules can be polymerized by electron beam irradiation [6]. Although as-grown C₆₀NWs are composed of the C₆₀ molecules that are weakly bonded via van der Waals forces [7], the C₆₀NWs irradiated by electron beams showed the stronger thermal stability [8], the higher Young's modulus [9] than pristine van der Waals C₆₀ crystals. Hence, it is of great importance to study the polymerization of C₆₀NWs in order to improve their mechanical and thermal properties.

Laser irradiation is a promising method to obtain the polymerized C₆₀ molecules [7, 10]. We first showed the photopolymerization of C₆₀NWs by using the Raman laser beam irradiation [7]. Rao et al. showed that the peak of A_g(2) pentagonal pinch mode of C₆₀ shifts downward from 1469 cm⁻¹ to 1459 cm⁻¹ upon the photopolymerization [11], showing that the shift of A_g(2) peak is a good indicator for the polymerization of C₆₀.

Alvarez-Zauco et al. studied the polymerization of C₆₀ thin films in air by the ultraviolet (UV) laser irradiation as a function of laser energy dose (= fluence) from 10 to

50 mJ/cm² in order to optimize the photopolymerization of C₆₀ films [12]. Likewise, the laser energy dose for the photopolymerization of C₆₀NWs should be optimized. Hence, the present study aims to reveal how the polymerization of C₆₀NWs proceeds as a function of the laser beam energy dose.

2. Experimental

C₆₀NWs were synthesized by a modified liquid-liquid interfacial precipitation method. Isopropyl alcohol (IPA) was gently poured into a toluene solution saturated with C₆₀ (MTR Ltd. 99.5%) in a glass bottle to make a liquid-liquid interface, and then the solution was subjected to ultrasonication and stored in an incubator at 10°C to grow short C₆₀NWs. The synthesized C₆₀NWs were filtered and dried in vacuum at 100°C for 120 min. to remove the solvents. In the Raman spectrometry analyses, the C₆₀NWs dispersed in ethyl alcohol were mounted on a slide glass and dried in air.

A Raman spectrometer (JASCO, NRS-3100) with a green laser of 532 nm excitation wavelength was used for the polymerization and structural analysis of C₆₀NWs in air. The power of laser light illuminated onto the specimens was measured by using a silicon photodiode (S2281, Hamamatsu Photonics K.K.). The laser beam power density (*D*) and

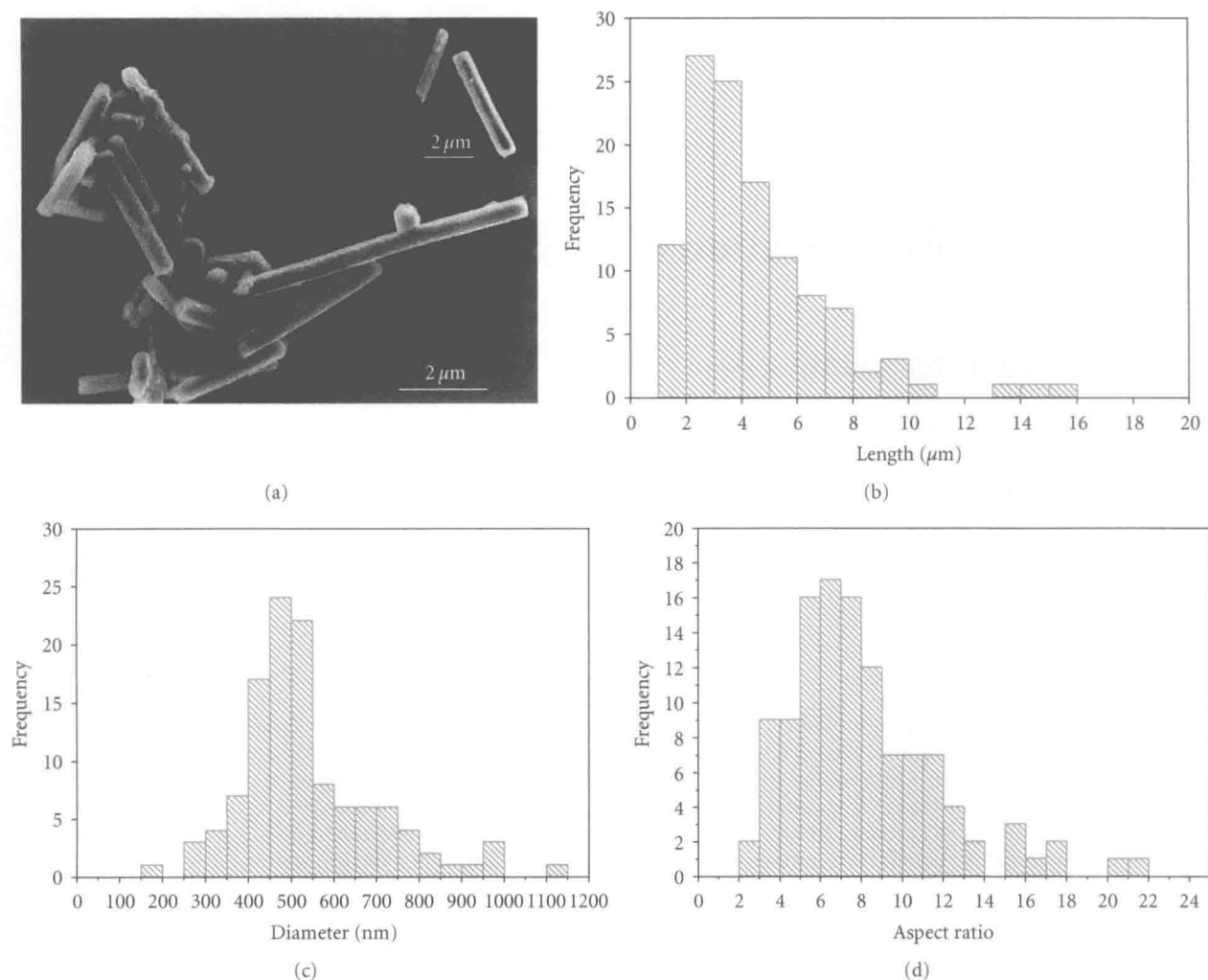


FIGURE 1: (a) SEM images, (b) length, (c) diameter, and (d) aspect ratio (length/diameter) distributions of the synthesized C₆₀NWs.

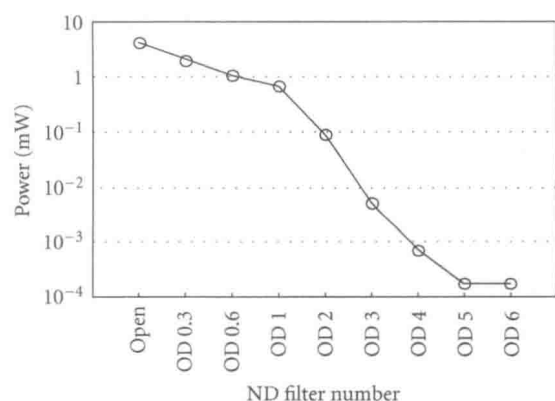


FIGURE 2: Relationship between the neutral density (ND) filter number and the laser beam power.

the energy dose of excitation laser beams in the Raman spectroscopy were controlled by changing ND (Neutral Density) filters, the defocus value of objective lens, and the

exposure time of laser beam. D is defined by the following formula in this paper,

$$D \text{ (mW/mm}^2\text{)} = \frac{\text{The power of laser beam (mW)}}{\text{the area of laser beam exposed on the sample (mm}^2\text{)}} \quad (1)$$

3. Results and Discussion

Figure 1 shows examples of scanning electron microscopy (SEM) images and the size distributions of the synthesized C₆₀NWs with a mean length of $4.4 \pm 2.7 \mu\text{m}$ and a mean diameter of $540 \pm 161 \text{ nm}$. The distribution of aspect ratios (length/diameter) is also shown. Most of the C₆₀NWs were found to possess the aspect ratios less than 15.

The power of excitation laser beam can be changed by selecting ND filters. Figure 2 shows the relationship between the ND filter number and the power of laser beam irradiated on samples. The laser beam power could be widely changed

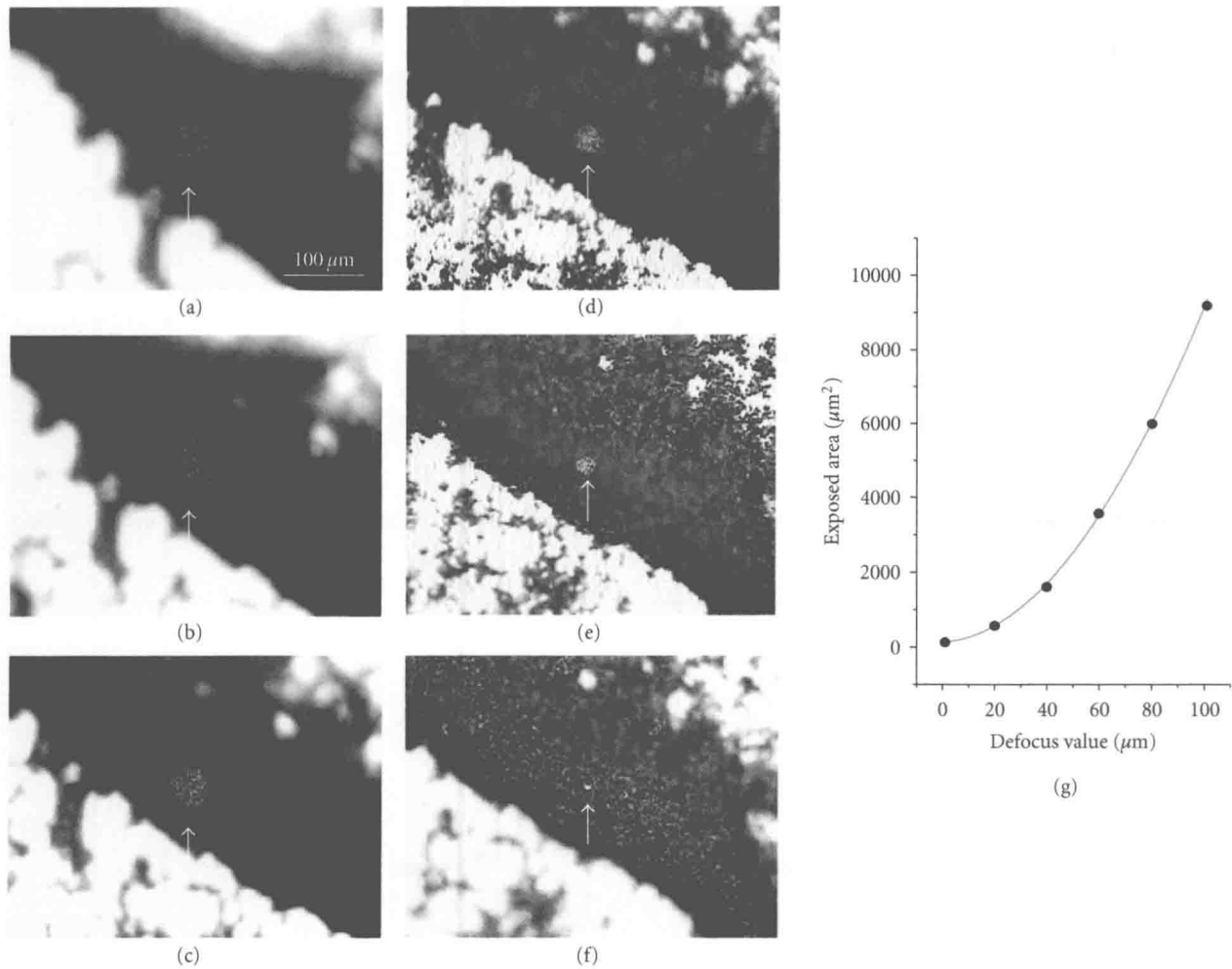


FIGURE 3: Optical microscopy images of the samples of C₆₀NWs irradiated by the excitation laser beams for the defocus values (under focus) of (a) 100, (b) 80, (c) 60, (d) 40, (e) 20, and (f) 0 μm and for the arrowed exposed areas of (a) 9270, (b) 6630, (c) 3480, (d) 1470, (e) 617, and (f) 63.8 μm², respectively. Graph (g) shows the relationship between the defocus value and the exposed area.

between OD1 and OD3. The ND filters OD1 (attenuation rate 0.1), OD2 (0.01), and OD3 (0.001) were used in the experiment, since the other filters gave too strong or too weak laser beam energies. The excitation laser beam power density could be varied from about 0.53 to 11800 mW/mm² using the above ND filters and by controlling the irradiation area of the laser beams and the defocus value from 0 to 100 μm as shown in Figure 3. The defocus value is defined as the distance from actual image plane and was set to be positive as the distance between the objective lens and the sample surface decreased. The places of C₆₀NWs exposed to the excitation laser beams can be recognized as the green circular areas marked in Figures 3(a)–3(f). The area of laser beam on the samples could be changed from 63.8 to 9270 μm² by controlling the defocus value from 0 to 100 μm.

The exposed area (y , μm²) and the defocus value (x , μm) were plotted as shown in Figure 3(g). The plotted points can be approximated by the fitted quadratic curve, $y = 0.88x^2 + 6.8x + 36$. Figure 4 summarizes the relationship among the laser beam power density, ND filter number, and the defocus value.

Figure 5 shows examples of the Raman spectra of C₆₀NWs taken by using the ND filters of OD1, OD2, and OD3 for an exposure time of about 220 s, where the spot size of laser beam on samples was 9 μm in diameter. Each power density of the excitation laser beam was (a) 11800, (b) 1660, and (c) 71.5 mW/mm², respectively. The A_g(2) peak around 1468 cm⁻¹ sifted to the lower wavenumbers with increasing the laser beam power density.

Figure 6 shows the A_g(2) peak positions of the Raman spectra of C₆₀NWs as a function of energy dose of the laser beam for each defocus value from 100 μm to 0 μm (just focus). The power density of laser beam on samples was changed by changing the defocus value and the ND filter number as shown in Figure 4. The energy dose was changed by setting the beam exposure time at 215 ± 6 s, 441 ± 10 s, 665 ± 9 s, and 899 ± 29 s for each power density. Hence, as a whole, 72 data points are plotted in Figure 6. As shown in Figure 5, the Raman shifts are found to generally decrease to the lower values with increasing the energy dose. However, the Raman shifts were observed to increase along

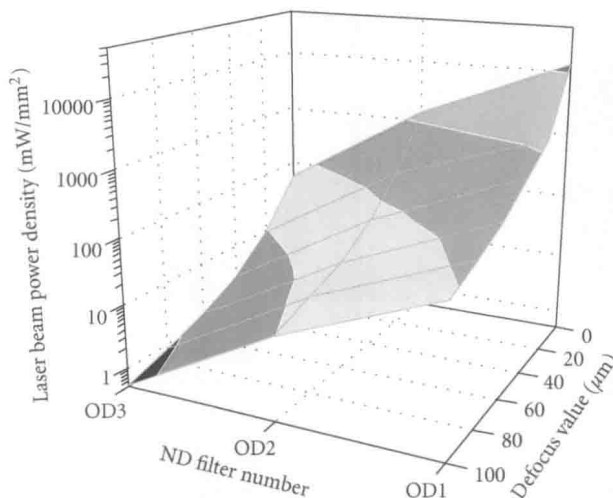


FIGURE 4: Power density of the Raman excitation laser beam measured as a function of ND filter number and the defocus value.

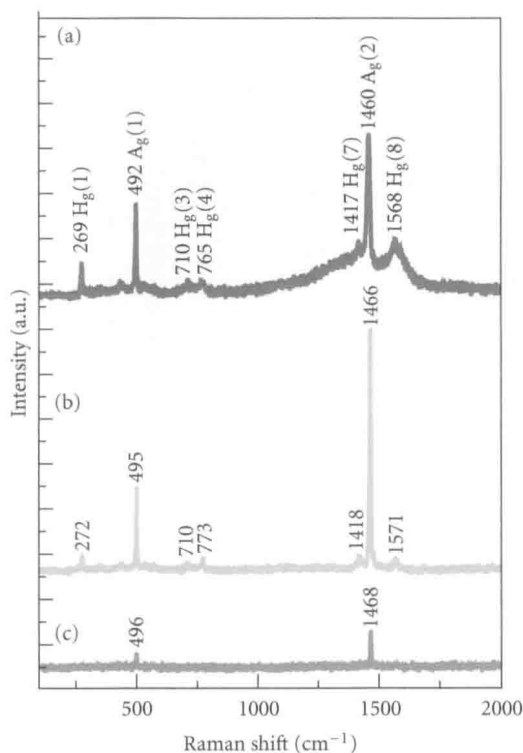


FIGURE 5: Raman spectra of C_{60} NWs. The power density of laser beam (D) is (a) 11800, (b) 1660, and (c) 71.5 mW/mm^2 , respectively.

the red arrows for the high energy doses in Figures 6(c), 6(d), 6(e), and 6(f). These phenomena are supposed to be explained by the temperature rise of the C_{60} NWs exposed to the laser beams, since it is known that the photopolymerized C_{60} molecules decompose into their primary monomers and dimers by heating at temperatures higher than about 100°C [13].

The data points obtained using the highest power densities are indicated in each graph of Figure 6 by the black arrows for the exposure time of about 220 s. Figure 7 shows the relationship between the laser beam energy dose

and the $A_g(2)$ peak position for the arrowed data points of Figure 6. The fitted curve of semilog plot is expressed as $y = -2.2x + 1467$, where x represents \log_{10} (laser beam energy dose) and y represents the Raman shift of $A_g(2)$ peak. Using this experimental formula, the energy dose more than about $1520 \text{ J}/\text{mm}^2$ is found to be necessary for the photopolymerization of C_{60} NWs in air, when the laser light with a wavelength of 532 nm is used.

Since it is known that the photopolymerization of C_{60} progresses through the formation of four-membered rings between adjacent C_{60} molecules [11], it is considered that

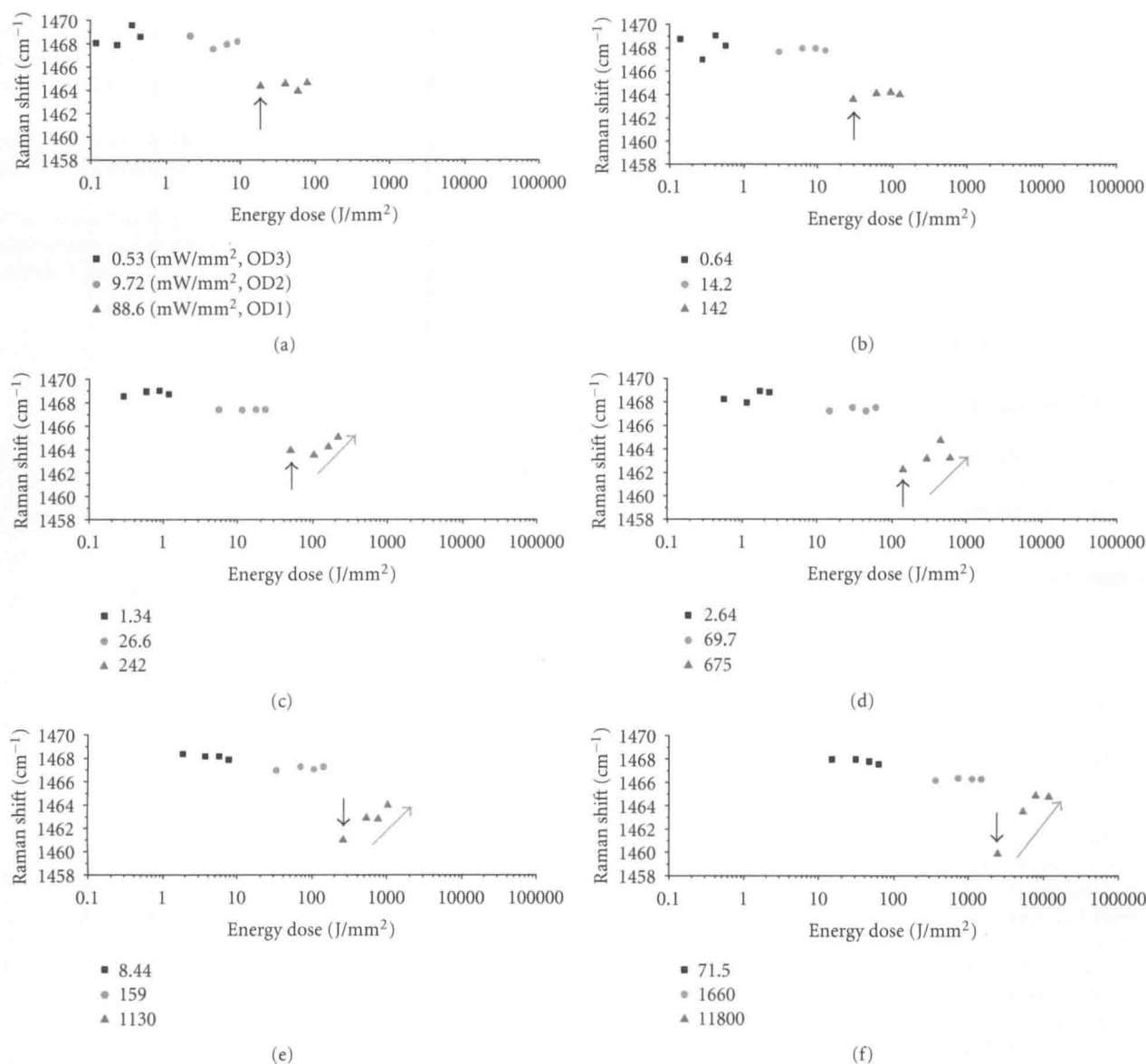


FIGURE 6: A_g(2) peak positions of the Raman spectra of C₆₀NWs under various exposure conditions at the defocus values of (a) 100 μm, (b) 80 μm, (c) 60 μm, (d) 40 μm, (e) 20 μm, and (f) 0 μm (just focus), corresponding to (a) ~ (f) of Figure 3.

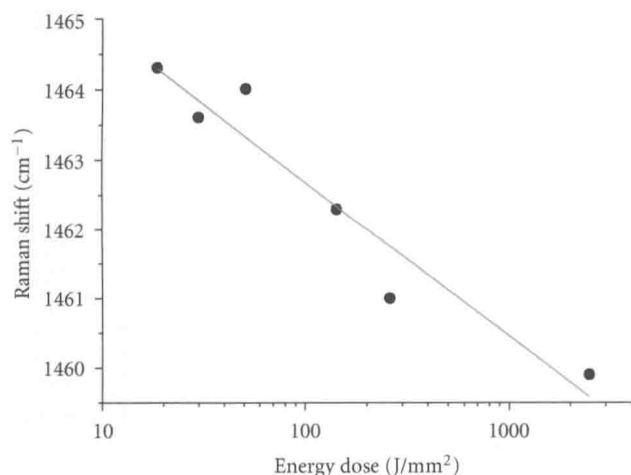


FIGURE 7: Relationship between the Raman shift of A_g(2) peak and the energy dose of C₆₀NWs irradiated by the excitation laser beams.

C₆₀ molecules are linearly polymerized by forming the four-membered rings along the growth axis of C₆₀NWs, as was shown in Figure 6 of [2].

In the gas chromatography-mass spectrometry (GC-MS) measurement of solvents contained in the C₆₀NWs that were prepared by use of toluene and IPA, the major residual solvent was toluene, and the content of IPA was very small compared with toluene [14]. Since the residual toluene of C₆₀NWs was measured to be about 0.2% after drying in an Ar atmosphere at 100°C for 30 min. [14], it is considered that the residual toluene of the vacuum-dried samples of C₆₀NWs in the present experiment is negligible and does not influence the Raman profiles.

4. Conclusions

The photopolymerization of C₆₀NWs was investigated by using the Raman laser beam of 532 nm wavelength at various

exposure conditions for the power density and the exposure time in air.

The $A_g(2)$ peak of C_{60} NWs shifted to the lower wavenumbers from that of the as-grown dried C_{60} NWs. However, the $A_g(2)$ peaks were found to move to the higher wavenumbers from the polymerized positions by the irradiation of laser beams for high energy doses at high-power densities, indicating the thermal dissociation of polymerized C_{60} molecules owing to the temperature rise.

An energy dose larger than about 1520 J/mm^2 was found to be necessary for the laser beam of 532 nm wavelength to obtain the photopolymerized C_{60} NWs.

Acknowledgment

Part of this research was supported by Health and Labour Sciences Research Grants (H21-Chemistry-Ippan-008) from the Ministry of Health, Labour, and Welfare of Japan.

References

- [1] K. Miyazawa, "Synthesis and properties of fullerene nanowhiskers and fullerene nanotubes," *Journal of Nanoscience and Nanotechnology*, vol. 9, no. 1, pp. 41–50, 2009.
- [2] K. Miyazawa, Y. Kuwasaki, A. Obayashi, and M. Kuwabara, " C_{60} nanowhiskers formed by the liquid-liquid interfacial precipitation method," *Journal of Materials Research*, vol. 17, no. 1, pp. 83–88, 2002.
- [3] K. Ogawa, T. Kato, A. Ikegami et al., "Electrical properties of field-effect transistors based on C_{60} nanowhiskers," *Applied Physics Letters*, vol. 88, no. 11, Article ID 112109, 3 pages, 2006.
- [4] P. R. Somani, S. P. Somani, and M. Umeno, "Toward organic thick film solar cells: three dimensional bulk heterojunction organic thick film solar cell using fullerene single crystal nanorods," *Applied Physics Letters*, vol. 91, no. 17, Article ID 173503, 3 pages, 2007.
- [5] X. Zhang, Y. Qu, G. Piao, J. Zhao, and K. Jiao, "Reduced working electrode based on fullerene C_{60} nanotubes@DNA: characterization and application," *Materials Science and Engineering B*, vol. 175, no. 2, pp. 159–163, 2010.
- [6] M. Nakaya, T. Nakayama, and M. Aono, "Fabrication and electron-beam-induced polymerization of C_{60} nanoribbon," *Thin Solid Films*, vol. 464–465, pp. 327–330, 2004.
- [7] M. Tachibana, K. Kobayashi, T. Uchida, K. Kojima, M. Tanimura, and K. Miyazawa, "Photo-assisted growth and polymerization of C_{60} "nano"whiskers," *Chemical Physics Letters*, vol. 374, no. 3–4, pp. 279–285, 2003.
- [8] K. Miyazawa, J. Minato, M. Fujino, and T. Suga, "Structural investigation of heat-treated fullerene nanotubes and nanowhiskers," *Diamond and Related Materials*, vol. 15, no. 4–8, pp. 1143–1146, 2006.
- [9] K. Asaka, R. Kato, K. Miyazawa, and T. Kizuka, "Buckling of C_{60} whiskers," *Applied Physics Letters*, vol. 89, no. 7, Article ID 071912, 3 pages, 2006.
- [10] D. Koide, S. Kato, E. Ikeda, N. Iwata, and H. Yamamoto, "Free electron laser-polymerization of C_{60} grown by liquid-liquid-interfacial precipitation method," *IEICE Transactions on Electronics*, vol. 94, no. 2, pp. 151–156, 2011.
- [11] A. M. Rao, P. Zhou, K. A. Wang et al., "Photoinduced polymerization of solid C_{60} films," *Science*, vol. 259, no. 5097, pp. 955–957, 1993.
- [12] E. Alvarez-Zauco, H. Sobral, E. V. Basiuk, J. M. Saniger-Blesa, and M. Villagrán-Muniz, "Polymerization of C_{60} fullerene thin films by UV pulsed laser irradiation," *Applied Surface Science*, vol. 248, no. 1–4, pp. 243–247, 2005.
- [13] Y. Wang, J. M. Holden, X. X. Bi, and P. C. Eklund, "Thermal decomposition of polymeric C_{60} ," *Chemical Physics Letters*, vol. 217, no. 4, pp. 413–417, 1994.
- [14] M. Watanabe, K. Hotta, K. Miyazawa, and M. Tachibana, "GC-MS analysis of the solvents contained in C_{60} nanowhiskers," *Journal of Physics: Conference Series*, vol. 159, no. 1, Article ID 012010, 2009.